Fibers and Polymers 2021, Vol.22, No.1, 19-29
DOI 10.1007/s12221-021-0036-8

ISSN 1229-9197 (print version)
ISSN 1875-0052 (electronic version)

Electrospun Skin Tissue Engineering Scaffolds Based on Polycaprolactone/Hyaluronic Acid/L-ascorbic Acid

Mahsa Janmohammadi[1], Mohammad Sadegh Nourbakhsh[2]*, and Shahin Bonakdar[3]

[1]*Department of Biomedical Engineering, Faculty of New Sciences and Technologies, Semnan University, Semnan 3513119111, Iran*
[2]*Faculty of Materials and Metallurgical Engineering, Semnan University, Semnan 3513119111, Iran*
[3]*National Cell Bank, Pasteur Institute, Tehran 1316943551, Iran*

(Received January 10, 2020; Revised March 28, 2020; Accepted March 31, 2020)

Abstract: Skin tissue engineering is an evolving method to reconstruct skin damages caused by disease, burn or trauma. In skin tissue engineering, scaffolds should prepare three-dimensional structure for skin cells. Electrospinning technique has been widely applied for producing nano/micro-scale fiber scaffolds in tissue engineering. In this study, electrospun scaffolds based on polycaprolactone (PCL) and hyaluronic acid (HA) containing L-ascorbic acid (AA) were fabricated. Morphology, contact angle, functional groups, biodegradability and drug release of the scaffolds were evaluated. L929 fibroblast cells seeded on nanofibrous scaffolds and cell attachment and viability were evaluated as well. According to the results, the fibers diameter were less than 180 nm and by adding hyaluronic acid, the hydrophilicity of scaffolds increased and degradation rate was adjusted. The encapsulation efficiency and successful release of ascorbic acid in nanofibrous scaffolds were demonstrated. According to the results, the cell growth, proliferation and adhesion of L929 fibroblast cells on the PCL/HA/AA scaffolds were enhanced in comparison with the PCL scaffold. Moreover, PCL/HA (80:20) containing 40 mg of AA nanofibrous scaffold could be potentially applied for skin tissue engineering.

Keywords: Polycaprolactone, Hyaluronic acid, Electrospinning, L-ascorbic acid, Skin tissue engineering

Introduction

Skin tissue engineering is developing as one of the ways to repair damaged skin tissue [1]. Since skin is not capable of regeneration, it is necessary to provide approaches that proper cells, biologic materials and signaling factors to target the cells [2].

Electrospinning technique has been favored to produce continuous fibers with nano- and micro-sized. In electrospinning technique, with appropriate parameters such as voltage, feed rate, distance and polymer concentration can be obtained smooth, flexible and strong fibers. Nanofibrous matrices have high surface-to-volume ratio that are capable of mimicking the extracellular matrix and boosting the cell adhesion [3-5]. The nanofibrous scaffolds can be controlled release of drug or bioactive molecules in tissue engineering applications [6]. Scaffolds play a crucial role in skin tissue engineering. The scaffolds create orientation and 3D structure for the cells to secrete the extracellular matrix that is a fundamental requirement in the skin tissue engineering [7,8]. Therefore, the proper identification of the matrix for skin tissue engineering leads to the development and use of multiple scaffolds derived from both natural and synthetic materials [9,10]. Natural and synthetic polymers-based scaffolds can be used due to versatile properties such as biodegradability, hydrophilicity, hydrophobicity, solubility, water absorption and etc. [11].

Polycaprolactone (PCL) is a synthetic semi-crystalline aliphatic polymer with low degradation rates, hydrophobicity, non-toxic degradation by-products, good biocompatibility, and FDA approval. Electrospun PCL scaffolds are widely used in tissue engineering are the ideal material to consider for the structural support of repairing skin tissue [12-14]. To deal with the pure PCL hydrophobicity and the lack of surface cell recognition sites, incorporation of natural polymers into PCL nanofibers make them suitable for cell adhesion, proliferation, and differentiation [15,16].

Hyaluronic acid (HA) is a linear polysaccharide and a key glycosaminoglycan of extracellular matrix. HA has excellent biocompatibility that is extremely attractive for body repair such as skin and wound-healing processes [17-19]. HA is soluble in water, therefore, has a poor water resistance. Electrospinning of pure HA is a problem and to overcome this drawback, blending with other polymers has been suggested [20].

Ascorbic acid is a water-soluble vitamin and a major antioxidant in human blood, which cannot be synthesized by human and; it plays a crucial role in the synthesis of collagen and proteoglycans [21,22]. Ascorbic acid can induce the skin repair and wound healing in humans [23]. Ascorbic acid is very unstable in unsuitable environments such as light and heat; in order to overcome the instability, the encapsulation or immobilization procedure has been offered [24]. In a study, electrospun nanofibers containing ascorbic acid and caffeine was used for wound dressing. In this study, polyvinyl alcohol nanofiber containing ascorbic acid and caffeine was prepared by electrospinning. The results showed that the ascorbic acid and caffeine encapsulated successfully in nanofibers and could be promising for wound healing [25]. Core/shell nanofibers containing L-

*Corresponding author: s_nourbakhsh@semnan.ac.ir

ascorbic acid/poly(vinyl alcohol)-chitosan were fabricated by coaxial electrospinning for transdermal delivery system. In core/shell structure, poly(vinyl alcohol) and chitosan were used as a shell and L-ascorbic acid was used as core. Release profile demonstrated that the scaffold with L-ascorbic acid can be suitable for transdermal drug delivery [26].

Chanda *et al*. fabricated polycaprolactone/chitosan/hyaluronic acid bilayered scaffold and seeded Vero cells in the scaffolds. The results showed that the presence of HA improves wound healing [27]. In another study, three-dimensional hyaluronic acid grafts with or without keratinocytes were prepared and implanted in full-thickness skin wounds in rats. The HA grafts demonstrated wound healing and reduced scar formation, which could be useful for skin wounds [28].

Another study explored the effect of ascorbic acid on temporomandibular joint disc cells seeded on non-woven poly(glycolic acid) scaffolds. According to the results, a medium concentration of ascorbic acid is more advantageous for cell to attachment to scaffolds and the production of extracellular matrix, collagen content, and aggregate modulus [29].

The present study aims to fabricate electrospun polycaprolactone and hyaluronic acid nanofiber scaffolds containing L-ascorbic acid at ambient temperature that could release the L-ascorbic acid to boost the biomechanical and biological features of skin tissue engineering.

Experimental

Scaffold Synthesis

Materials

Polycaprolactone (PCL, Mn 80000) was purchased from Sigma-Aldrich. Hyaluronic acid (HA, Mw=1200 kD) was purchased from Nano Zist Arrayeh Pasteur Institute in Iran. L-ascorbic acid (AA, molar mass: 176.12 g/mol) and 1-Ethyl-3-(3-dimethylaminopropyl) carbodiimide (EDC) were purchased from Merck. Formic acid (FA, 100 %) and acetic acid (AA, 100 %) were purchased from Merck.

Polymer Solution Preparation

PCL solution (8 %) in formic acid/acetic acid (volume ratio 70:30) was prepared for the fabrication of PCL fibers. Solutions of polycaprolactone and hyaluronic acid (8 %) with weight ratios of (90:10), (85:15), (80:20) and PCL/HA (weight ratios of (100:0), (90:10), (85:15), (80:20)) with L-ascorbic acid (40 mg or 0.04 gr) was dissolved in a mixture of 70:30 formic acid and acetic acid and stirred for 6 h (Figure 1). The compositions of nanofibrous mats are shown in Table 1.

Electrospinning Conditions

The solutions were moved to a 5 m*l* syringe using blunt tipped stainless steel needles. A voltage of 15 kV and a flow rate 0.1 m*l*/h were applied. A 10-cm distance was maintained

Table 1. Compositions of nanofibrous mats

Scaffold	Polycaprolactone (%)	Hyaluronic acid (%)	L-ascorbic acid (mg)
S_1	100	-	-
S_2	90	10	-
S_3	85	15	-
S_4	80	20	-
S_5	90	10	40
S_6	85	15	40
S_7	80	20	40

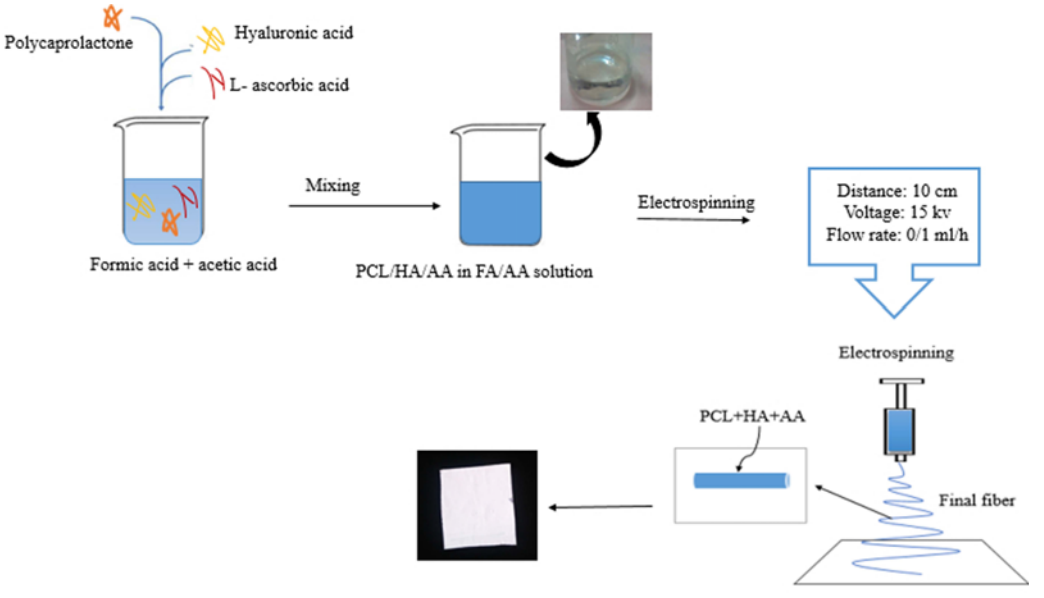

Figure 1. Schematic of electrospun scaffolds preparation.

between the needle tip and the collector. Fibrous mats collected on aluminum foil sheet were put to dry at 30 °C for 24 h in the oven.

Scaffold Crosslinking

The crosslinking was done using a 10 m*l* crosslinking medium. The PCL/HA and PCL/HA/AA fibrous scaffolds were immersed in a 50 mM EDC (1-Ethyl-3-(3-dimethylaminopropyl) carbodiimide) solution (ethanol to water is 8/2) and kept for 24 h at room temperature. Then, water and ethanol were used to wash the crosslinked scaffolds three fold, which were put to dry in oven at 25 °C for three days for removing the residual solvents.

Characterization of Electrospun Scaffolds

Scanning Electron Microscopy

The morphologies of electrospun PCL, PCL/HA and PCL/HA/AA fibrous scaffolds prior to and after crosslinking tests were explored using scanning electron microscope (SEM, XL30 Philips). The sputter coater was used to gold coat the samples prior to SEM analysis. Average fiber diameter was calculated using Image J software (Wayne Rasband, National Institute of Health, USA). The fiber diameter was logged as the average of three replicates.

FTIR Analysis

For assessing the chemical composition of scaffolds, Fourier Transform Infrared Spectroscopy (FTIR) analysis was carried out and the spectra were logged using Shimadzu-FTIR 8400S spectrophotometer. The FTIR spectra were prepared for the scaffolds prior to and following cross-linking with a spectral width ranging from 400-4000 cm^{-1}.

Ascorbic Acid Loading and Release

AA-loaded PCL-HA fiber mats (before cross-linking) were cut and weighed (around 20 mg) and immersed in 10 m*l* of 7:3 FA/AA. The amount of dissolved AA was determined using a UV spectrophotometer (UV-1650PC-SHIMADZU) at 262 nm, respectively. The results were recorded as average values (n=3). The following formula was applied for determining the encapsulation efficiency (%):

$$\text{Encapsulation efficiency (\%)} = (\text{Actual drug content})/(\text{Theoretical drug content}) \times 100$$

Actual drug content is the quantity of drug removed from the scaffold; theoretical drug content is the total of the drug added in the solution for electrospinning.

Three samples were immersed into 5 m*l* of fresh PBS solution at 37 °C. At predefined intervals, 1 m*l* of the test medium was removed and an equal amount of fresh PBS was added. Over 14 days, a sample was removed and the absorbance measured. The solutions were analyzed using a UV-1650PC-SHIMADZU spectrophotometer at 262 nm.

Contact Angle Measurements

For exploring the hydrophilicity of various nanofibrous scaffolds, contact angles were specified using a contact angle system CA-ES10. For each sample, water drops were put on the surface layers of the scaffolds. The contact angle was specified as the average of at least three measurements (n=3).

In vitro Degradation and Water Uptake

Prior to and following the crosslinking, fibrous scaffolds were dipped in 5 m*l* of PBS (pH 7.4) at 37 °C for different intervals. The degradation rate was assessed through the weight variations prior to and following dipping based on equation below:

$$\text{Weight loss (\%)} = (W_i - W_t)/(W_t) \times 100$$

where W_i matches the initial weight of the sample and W_t to the weight of the sample at time t.

The equilibrium water contents of scaffolds were individually determined in distilled water at room temperature for 24 h at 25 °C. The water uptake (%) was determined using the following equation:

$$\text{Water uptake (\%)} = (W_t - W_0)/W_0 \times 100$$

where W_t denotes the weight of the wet membrane determined at 24 hours, and W_0 denotes the weight of the dry membrane determined at time 0.

Evaluation of Mechanical Properties

Mechanical features of scaffolds were assessed at room temperature. Scaffolds were cut into 1×3 cm^2 pieces, fixed into a tensiometer (Tensile/Bending/Compression Zwick/Roell Z050) and tested through the application of a load cell of 50 N at a tensile loading rate of 20 mm/min^{-1}. The mechanical features of the scaffolds were determined based on the ultimate tensile strength (UTS), strain at break (ε) and Young's modulus (E). Each data point shows the average of three replicates.

Cell Response to Scaffolds

Viability Analysis

PCL, PCL/HA and PCL/HA/AA nanofibrous scaffolds were exposed to UV radiation and then washed with PBS before cell seeding. L929 fibroblast cells were isolated and cultured in RPMI media with 10 % FBS. 1×10^4 cells were seeded onto scaffolds in 12 well plates and incubated for 24 hours at 37 °C. The culture media were kept at 37 °C under 5 % CO_2 by replacing with the fresh media every 3-4 days. Then, after removing the culture medium, 400 μ*l* MTT was added to each well of plate and incubation was done for 4 hours. After careful removal of MTT solution from each well, they were replaced by isopropanol. Then, an ELISA reader was applied to record (STAT FAX 2100, USA) the absorbance of solution at 570 nm. The MTT assay was carried out after 3 and 7 days of cell culture on PCL, PCL/HA and PCL/HA/AA scaffolds to evaluate cell proliferation rate of L929 fibroblast cells. Experiments were done in triplicate.

Cell Attachment

Nanofibrous scaffolds were used in 6-well plates. 20000 cells were seeded onto scaffolds and incubated for 5 hours at 37 °C. Culture media with 10 % FBS was added and after 24 h of culturing, all media was removed from culture plates and each well was washed with PBS. 3.5 % glutaraldehyde (GA) was applied for fixing the samples for 2 h. Then, PBS and deionized water were used to wash the samples. Next, SEM was used to explore the morphology of cells on the scaffolds.

Statistical Analysis

The statistical analysis was done on the means of the data obtained from at three replicates. All data were expressed as mean±standard deviation. A p value of <0.05 was set statistically significant.

Results and Discussion

Characterization of Nanofibrous Scaffolds

SEM

SEM images and average diameter of the nanofibrous scaffolds are shown in Figure 2. The scaffolds were composed of uniform bead-free fibers. According to the images, the pores were interconnected that contributed to cell penetration and cell-ECM interaction. On average, the fibers of all samples were less than 180 nm in diameter that was reduced by increased hyaluronic acid ratio. No significant difference was observed between the PCL/HA/AA and PCL/HA scaffolds fiber diameters (Figure 2). Fiber diameter of PCL, PCL/HA (90:10) (85:15) (80:20) scaffold was 169±6, 114±6, 92±5 and 89±4, respectively. The diameter of PCL/HA (90:10) containing 40 mg of AA, PCL/HA (85:15) containing 40 mg of AA and PCL/HA (80:20) containing 40 mg of AA scaffolds was 95±4, 87±4 and 83±3 nm, respectively. Fiber diameter of PCL/HA and PCL/HA/AA scaffolds were significantly lower than PCL scaffold.

SEM images of the crosslinked nanofibrous scaffolds are shown in Figure 3. HA is very hydrophilic and water soluble, which is necessary to crosslink to obtain a water resistant material in aqueous mediums. Nanofibrous scaffolds were cross-linked with EDC [30-32]. The SEM images demonstrated that the structure of the PCL/HA/AA and PCL/HA scaffolds was largely preserved after crosslinking

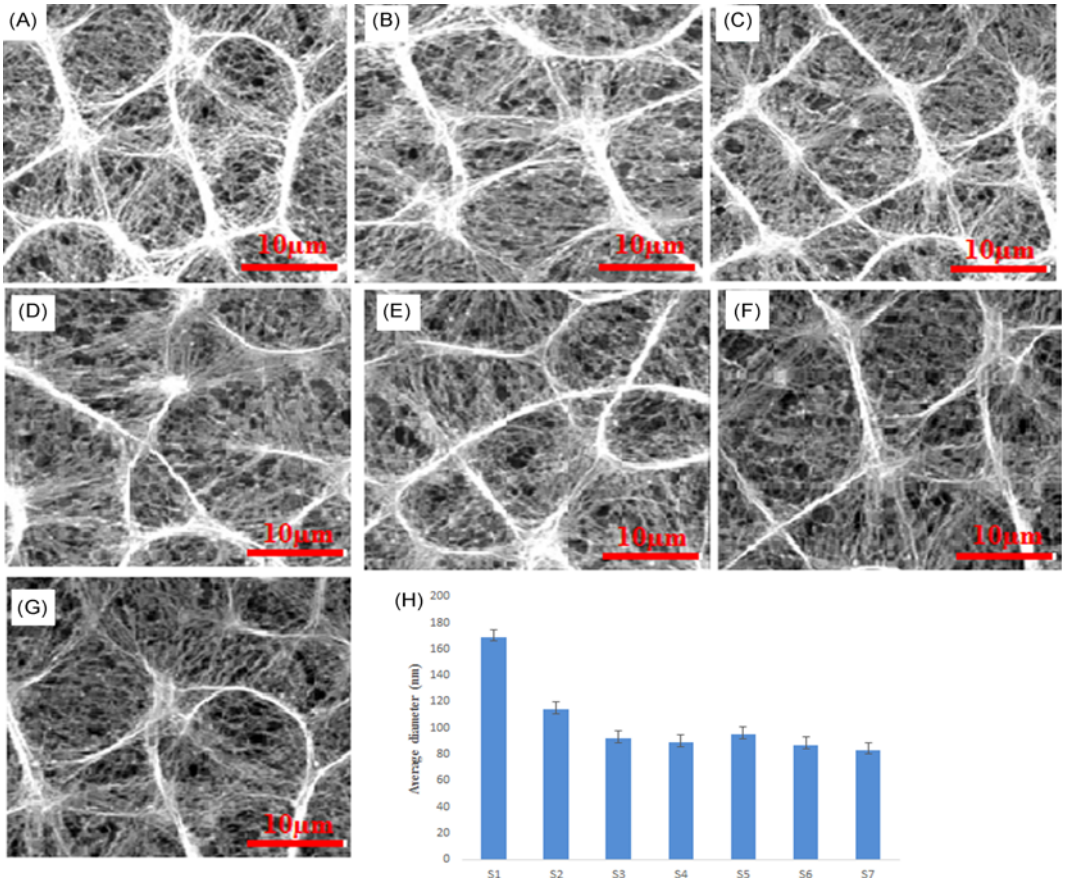

Figure 2. Morphology of nanofibrous scaffolds (A-G): (A) PCL, (B) PCL: HA (90:10), (C) PCL: HA (85:15), (D) PCL: HA (80:20), (E) PCL: HA (90:10) containing 40 mg of AA, (F) PCL:HA (85:15) containing 40 mg of AA, (G) PCL: HA (80:20) containing 40 mg of AA. (H) fiber diameters of the scaffolds.

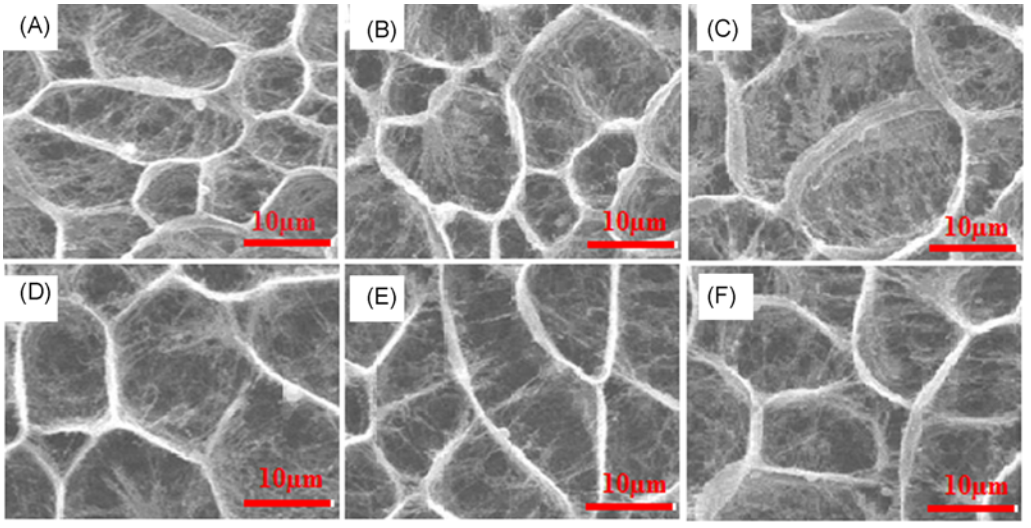

Figure 3. Morphology of crosslinked nanofibrous scaffolds; (A) PCL: HA (90:10), (B) PCL: HA (85:15), (C) PCL: HA (80:20), (D) PCL: HA (90:10) containing 40 mg of AA (E) PCL: HA (85:15) containing 40 mg of AA, and (F) PCL: HA (80:20) containing 40 mg of AA.

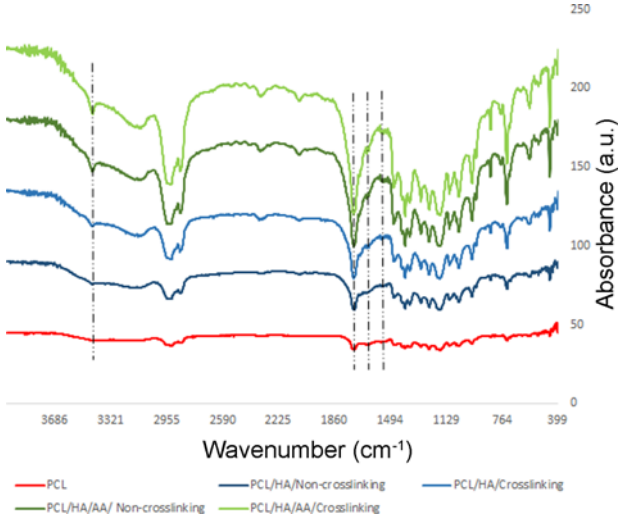

Figure 4. FTIR analysis of electrospun nanofibrous scaffolds; (A) PCL, (B) PCL/HA before and after crosslinking, and (C) PCL/HA/AA before and after crosslinking.

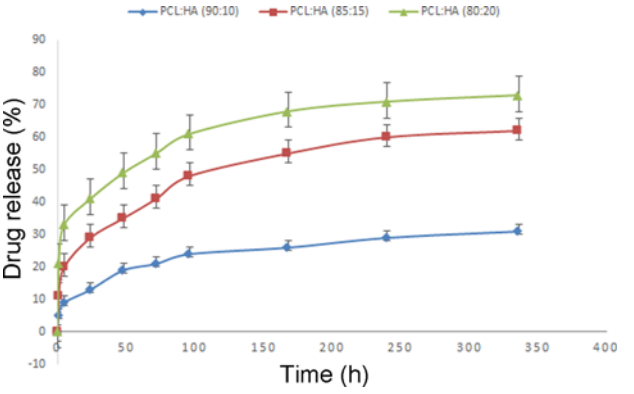

Figure 5. Cumulative release of ascorbic acid from scaffolds over 14 days ($p<0.05$).

in the presence of EDC and only small degree of swelling between fibers and little changes after crosslinking were observed.

Functional Group Characterization

The FTIR spectra of PCL, PCL/HA and PCL/HA/AA blends are shown in Figure 4. The infrared absorption characteristic peaks of PCL were observed of asymmetric -CH_2-stretching at 2929 cm^{-1}, symmetric-CH_2-stretching at 2866 cm^{-1} and carbonyl stretching at 1731 cm^{-1}. Infrared spectra of blended PCL/HA scaffolds displayed absorption peaks of O-H stretching bond and amino group (3436 cm^{-1}). The absorption peaks at 1650 cm^{-1}, 1633 cm^{-1} and 1537 cm^{-1}, 1533 cm^{-1} shows the presence of amid I group and amid II group prior to and following the crosslinking. AA in PCL/HA/AA scaffold has an absorbance peak at 1693 cm^{-1}, 1687 cm^{-1} and 1396 cm^{-1}, 1363 cm^{-1} of C=C and -CH-stretching bonds prior to and following the crosslinking.

Encapsulation Efficiency and Release of AA

The actual amount of the AA incorporated in the PCL/HA fibers before crosslinking was calculated. The actual amounts of AA in the PCL/HA fibers (90:10) (85:15) (80:20) were 36±3 %, 60±7 % and 83±6 %. The amount of AA in the PCL/HA (80:20) demonstrated that AA was encapsulated well within the fiber. The AA release profiles from the cross-linked fibers over 14 days are depicted in Figure 5. Within the first 24 h, 13 %, 29 % and 41 % of ascorbic acid were released from PCL/HA (90:10) (85:15) (80:20) fibrous mats, respectively Approximately, 31 %, 62 % and 73 % of AA was gradually released by 336 h of PCL/HA (90:10) (85:15) (80:20) scaffolds.

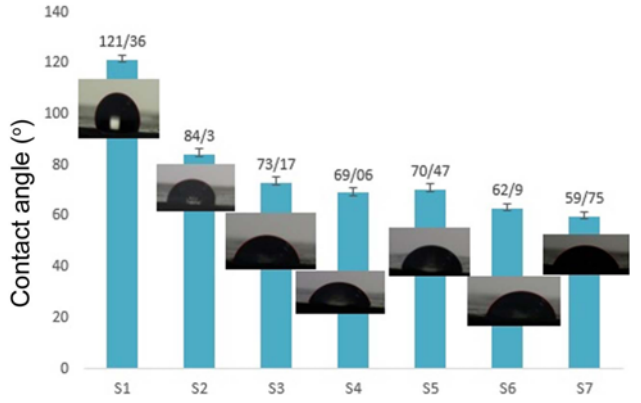

Figure 6. Water contact-angle measurements of electrospun nanofibrous scaffolds.

Water Contact-angle Measurements

Figure 6 shows the water contact-angle measurements of PCL, PCL/HA and PCL/HA/AA scaffolds. PCL is hydrophobic and the PCL scaffold displayed a contact angle of 121.36°. The PCL/HA scaffolds displayed a reduction in contact angles because of the presence of hydrophilic HA molecules and water contact-angle decreased by increasing hyaluronan content. The presence of hydrophilic groups of AA in the structure decreased water contact-angle and increased hydrophilicity.

In vitro Degradability and Water Absorption of Crosslinked and Non-crosslinked Fibrous Scaffolds

Results of the degradation test over a period of 30 days are shown in Figure 7(a, b). PCL is hydrophobic, and to adjust the biodegradability of PCL fibrous scaffold, HA was added. PCL scaffold lost approximately 1.8 % of its weight after 30 days. Compared to pure PCL fibrous scaffold, the degradation time of HA/PCL fibrous scaffolds decreased greatly from days. The more the HA content, increased the degradation rate. When AA was incorporated into scaffolds, the degradation rate of scaffolds was increased. The crosslinked fibrous scaffolds were much more stable than non-crosslinked fibrous scaffolds in PBS. The swelling test for crosslinked fibrous scaffolds in the PBS, as expected given the lower degradation and the EDC is able to diffuse efficiently throughout the HA and cross-link the HA molecules. This result confirmed successful HA cross-linking following the electrospinning process, which kept bonding for more than the time for non-crosslinked fibrous scaffolds. The water absorption of the scaffolds are indicated in Figure 7(c). PCL scaffold exhibited low water absorption. Water absorption increased with increasing the hyaluronan content and presence of AA. This result could be linked with high water absorption by the hyaluronic acid of the fibrous scaffold.

Mechanical Properties

Mechanical properties of the scaffolds were measured and

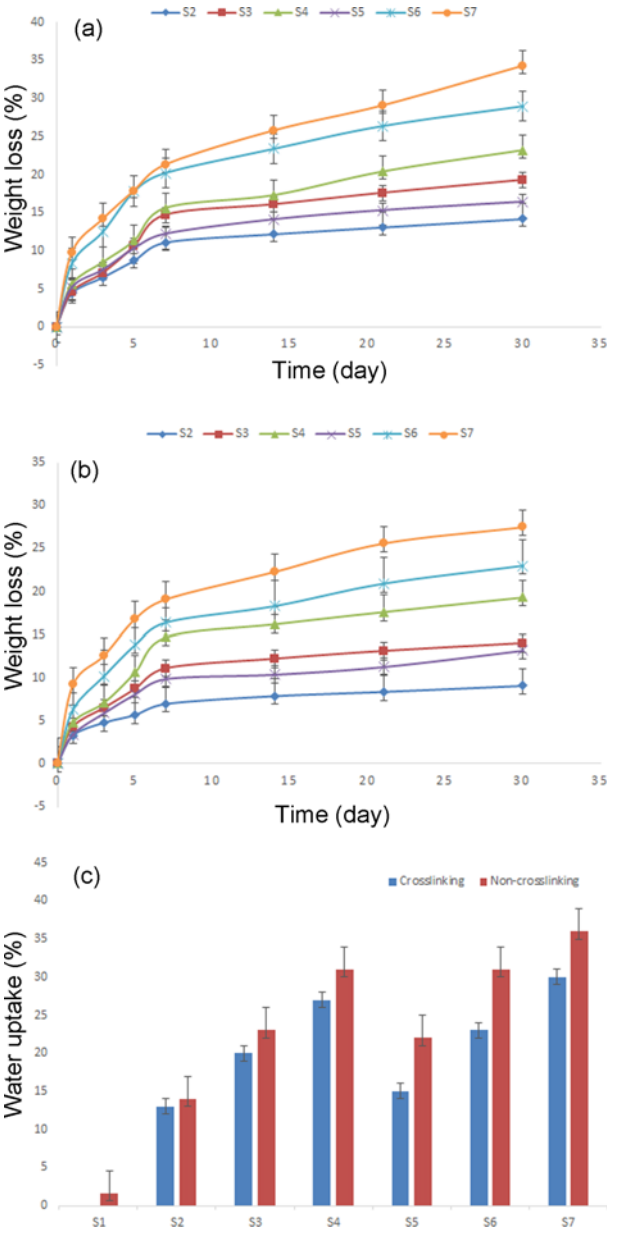

Figure 7. Evaluation of weight loss of electrospun nanofibrous scaffolds for 30 days; (a) before crosslinking, (b) after crosslinking ($p<0.05$), and (c) water sorption of nanofibrous scaffolds.

reported in Figure 8. The PCL scaffold ultimate tensile stress and Young's modulus were significantly higher than the PCL/HA scaffolds. HA is poor in terms of biomechanical features, thus, tensile stress and Young's modulus was almost reduced for PCL/HA in comparison with the pure PCL scaffold. PCL/HA/AA scaffolds had roughly higher ultimate tensile stress and Young's modulus values in comparison with PCL/HA scaffolds. The controlled and sustained release of incorporation of these forms of ascorbic acid increased the strength.

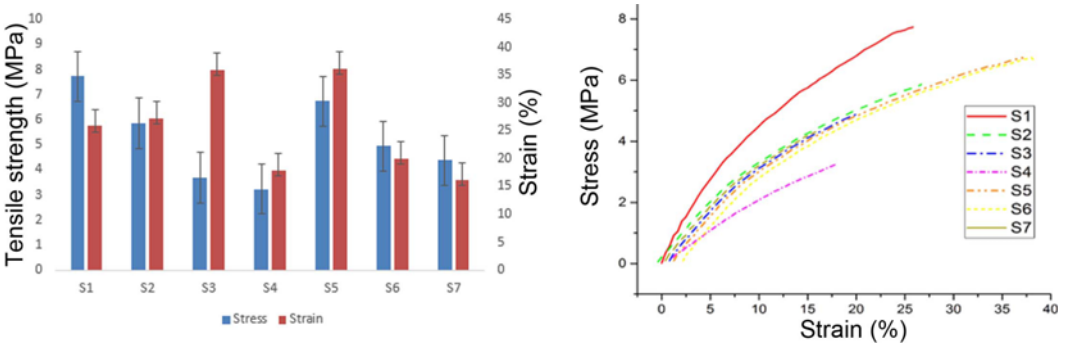

Figure 8. Representative tensile strength curves of electrospun nanofibrous scaffolds.

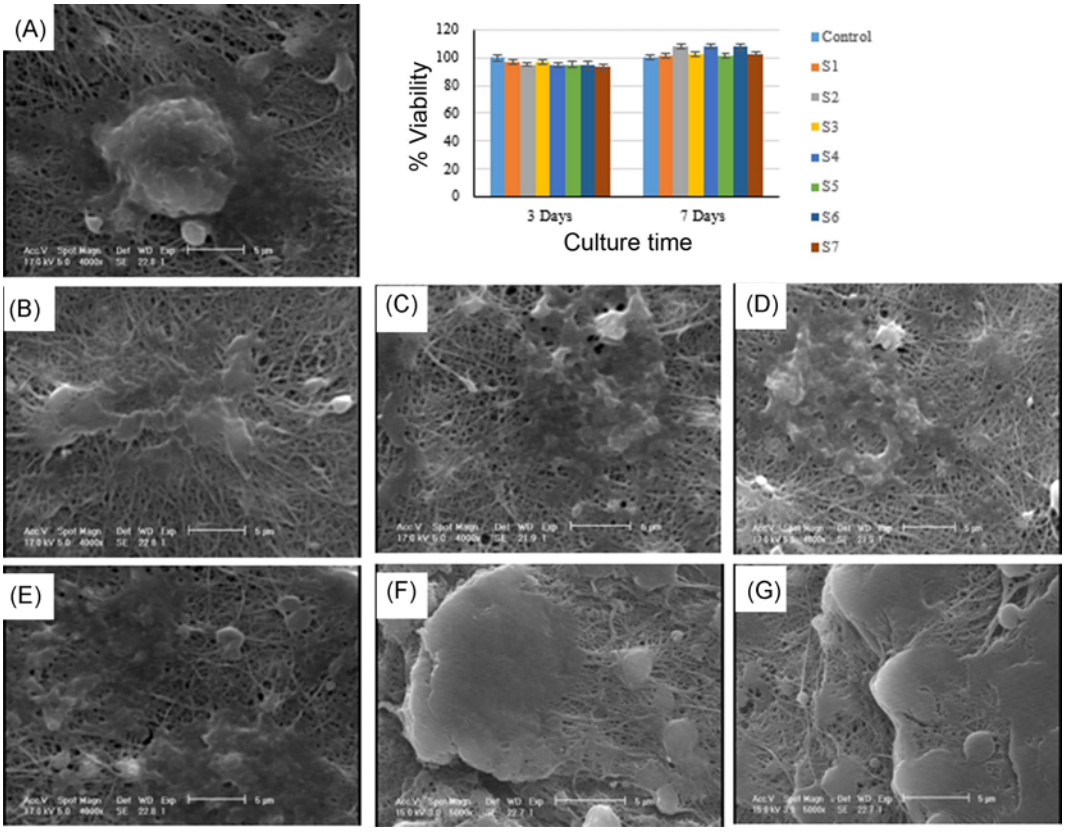

Figure 9. MTT analysis of scaffolds for 3 and 7 days (upper right graph), (A-G) attachment of L929 fibroblast cells into nanofibrous scaffolds, (A) PCL, (B) PCL:HA (90:10), (C) PCL:HA (85:15), (D) PCL:HA (80:20), (E) PCL: HA (90:10) containing 40 mg of AA, (F) PCL: HA (85:15) containing 40 mg of AA, and (G) PCL:HA (80:20) containing 40 mg of AA.

Cell Viability and Adhesion

The MTT assay results are given in Figure 9(upper right graph). The results showed that all scaffolds were nontoxic; furthermore, the cell viability was increased compared to the control sample after 7 days. Figure 9(b), shows the morphology of L929 fibroblast cells on the scaffolds. SEM images of cell growth on the PCL/HA and PCL/HA/AA electrospun scaffolds showed higher cell proliferation compared with pure PCL scaffolds. These results demonstrated cellular attachment of L929 fibroblast cells on all the electrospun scaffolds, and cell attachment on the PCL//HA (80:20) containing 40 mg of AA sample was clearly better than the other samples.

The polycaprolactone/hyaluronic acid/L-ascorbic acid nanofibrous scaffolds were successfully developed via electrospinning for skin tissue engineering applications. The aim of this study L-ascorbic acid releasing from biodegradable nanofibrous scaffolds and ascorbic acid with hyaluronic acid

stimulate skin repair and new tissue formation. Nanofibrous scaffolds were evaluated by the SEM analysis before and after crosslinking. Scaffolds were fabricated with uniform structure without beads. The results revealed that the change in the polymers ratio and solution influenced the fiber size. The average fiber diameter was decreased by increasing the hyaluronic acid content because HA in the high voltage electric field increasing the electrostatic force and the fiber diameter would decrease. Formic acid with high dielectric constant decreased the diameter of the fibers [33,34]. Earlier studies on polycaprolactone and hyaluronic acid electrospun fibers also showed that the incorporation of hyaluronic acid in polycaprolactone solution considerably reduced the diameter of electrospun fibers [35]. Another study applied the electrospinning method to investigate the pure poly-lactic acid scaffold and poly-lactic acid/L-ascorbic acid, ascorbate-2-phosphate scaffold. According to the results, the fiber diameter and pore size of L-ascorbic acid, ascorbate-2-phosphate and poly-lactic acid scaffolds were not different significantly [36]. HA is water soluble and EDC was reactive with the carboxyl groups of HA and was biocompatible and nontoxic [37,38]. Cross-linking after the electrospinning process with EDC which leads to HA insoluble in water [20]. Similarly, in another study, the electrospun gelatin and hyaluronan - gelatin fibers cross-linked with EDC for nerve tissue engineering and the fiber morphology showed that the gelatin and hyaluronan-gelatin fibers still maintained their morphology after crosslinking [39].

To determine the characteristic peaks of scaffolds, FTIR analysis was performed. FTIR showed the characteristic absorbance peak for PCL scaffold [40,41]. The PCL/HA and PCL/HA/AA scaffolds were evaluated. All scaffold groups showed the characteristic peaks for HA [42-44] and AA [45-48]. Ascorbic acid is a potent antioxidant, which promotes collagen biosynthesis, scavenges free radicals; thus, the encapsulated ascorbic acid within the polymeric matrix should have significantly higher efficiency [49,50]. The result showed that electrospun scaffolds were able to encapsulate and release AA with in the polymers successfully.

Contact angle results showed that PCL scaffold was 121.36^{o} [51], while after adding HA and AA, the scaffolds contact angle decreased [52,53]. Polycaprolactone is hydrophobic but by adding hyaluronic acid and ascorbic acid, the contact angle decreased because hydrophilic group could enhance hydrophilicity. In a study, PCL/PMMA scaffold was fabricated for bone tissue engineering. According to the result of contact angle, the contact angle of the PCL scaffold was $110.0^{o}\pm0.3^{o}$. PCL scaffold showed hydrophobic behavior was brought about by the CH_3 groups and with incorporation of poly(methyl methacrylate), the contact angle reduced to $95.0^{o}\pm0.4^{o}$ for the 3/7 PCL/PMMA [54]. In another study, polycaprolactone/silk fibroin/hyaluronan scaffolds were fabricated via emulsion electrospinning. Water contact angle was investigated; electrospun PCL fibers contact angle was 128 ± 8^{o}. With incorporation of SF and HA, scaffolds became more hydrophilic and decreased the contact angle [55]. Chanda *et al*. assessed the hydrophilicity and water retention ability of CS/PCL-HA. According to the contact angle results, following the addition of HA, the hydrophilicity capacity of PCL and CS/PCL scaffolds increased considerably by decreased contact angle [27]. Gandhimathi *et al*. fabricated polycaprolactone (PCL), silk fibroin (SF), ascorbic acid (AA) and dexamethasone (DM) by the electrospraying for bone tissue engineering [56].

In vitro degradation of scaffolds was evaluated over thirty days. The degradation of PCL/HA and PCL/HA/AA scaffolds was higher than PCL scaffold. HA could enhance the biodegradability of scaffolds because hyaluronic acid was hydrophilic [57,58]. To reduce the rapid removal of hyaluronic acid, the scaffolds were cross-linked. The results showed that degradability of non-crosslinked scaffold was higher than crosslinked scaffolds. In a study, a bilayered electrospun membrane was fabricated. The upper layer of the membrane consisted of hyaluronic acid/polycaprolactone and chitosan/zein were applied for building the bottom layer. To explore the degradation behavior, the scaffolds were dipped in PBS. The degradation rates of polymeric matrices were calculated after 1, 3 and 7 days. PCL displayed a slow degradation profile and HA polymers showed an organized biodegradability. According to the degradation results, HA/PCL membrane lost roughly 5 % of its weight after 7 days because of the presence of PCL. Furthermore, CS/ZN/SA membrane showed the highest weight loss after 7 days and the electrospun bilayer membrane lost almost 10 % of its weight after 7 days [59].

In another study, the degradation rate was determined for polycaprolactone, polycaprolactone/chitosan and polycaprolactone/ chitosan/hyaluronic acid scaffolds. The results confirmed the decreased rate of degradation for PCL and adding HA boosted degradation rate of CS/PCL-HA in comparison with PCL and CS/PCL scaffolds after 15 days of immersion in PBS [27]. The water absorption of scaffolds was evaluated for 24 h. The water-absorptive swelling was expected to impart a hydrogel-like nature and affect the transfer of cell nutrients and metabolites. Increasing the hydrophilicity of scaffolds improved the cell adhesion and proliferation [60]. The results showed that PCL/HA and PCL/HA/AA scaffolds had a higher water absorption than the PCL scaffold. Water absorption analysis of polycaprolactone and polycaprolactone/hyaluronic acid (PCL-HA1s, PCL-HA2s) scaffolds were calculated in distilled water after 48 h. PCL-HA1s was a gel-like phase within the scaffold and, PCL-HA2s was a thin HA layer coating internal surfaces of PCL structure. The water absorption result showed HA coating led to increased equilibrium water content compared to PCL [61]. In another study, anti-adhesion barrier film was fabricated using hyaluronic acid-grafted electrospun poly

(caprolactone) nanofibrous membranes. The equilibrium water contents of PCL and PCL-g-HA NFMs were assessed in DDI water at 25 °C. Because of hydrophobicity of PCL, it was possible to use HA. According to the results, the water uptake increased 2.6 % to 30.6 % by the grafting of HA molecules to PCL NFM [42].

The tensile strength of PCL and PCL/HA/AA shows more than PCL/HA scaffolds. HA is weak in terms of mechanical properties [62] and PCL/HA scaffolds showed lower tensile strength. In a study, hybrid scaffolds were fabricated using hyaluronic acid (HA)-based hydrogel combined with porous poly(ε-caprolactone) (PCL) material. According to the results, the hybrid scaffolds increased loss modulus compared to PCL control scaffolds [63]. In another study by Ghosal *et al.*, electrospinning approach was applied for fabrication of polycaprolactone with titanium dioxide, also, nanofibers coated with collagen. The results showed that the polycaprolactone nanofibers can enhance mechanical strength, whereas the scaffold mechanical strength decreased in the presence of collagen to some extent [64]. Polycaprolactone with L-ascorbic acid 2-phosphate magnesium was fabricated via emulsion and blend electrospinning. Mechanical strength of the scaffolds showed the decrease in both tensile stress and the strain at break for emulsion electrospun scaffold compared with blend electrospun scaffold and polycaprolactone/L-ascorbic acid 2-phosphate magnesium displayed sufficient mechanical support [65].

The cell viability of PCL/HA/AA scaffolds was compared with other scaffolds and the results showed that better cell growth and cell adhesion. Several researchers have found that HA increases the cell growth and proliferation [66,67]. Some studies reported that hydrophilic substrates increased adhesion, spreading and growth of cells than hydrophobic or very hydrophilic substrates [60]. Selection of appropriate materials in polycaprolactone scaffold could improve wettability, biocompatibility, cell viability and cell adhesion [68]. In addition, studies have shown that the addition of AA increases the cell proliferation and adhesion of fibroblasts. Therefore, improved cell-scaffold interactions than the PCL scaffolds. In a study, aligned and random PCL fibers were fabricated through electrospinning and coating with chitosan-hyaluronic acid hydrogel. The cell viability studies showed the highest cell viability and cytocompatibility. Cell attachment results show that rabbit ligament fibroblasts cells have grown and attached well on scaffolds [69]. Some studies reported the effects of AA in cell growth. A study demonstrated that AA stimulated mesenchymal stem cells proliferation, differentiation and ECM secretion [70]. In another study, ascorbic acid released from lysine-di-isocyanate/glycerol/polyethylene glycol supported cell proliferation, type I collagen, and alkaline phosphatase synthesis in vitro [71]. Poly(l-lactic acid)-co-poly-(ε-caprolactone)/silk fibroin/tetracycline hydrochloride with ascorbic acid scaffold were fabricated via electrospinning. The results showed that AA-blended scaffolds stimulate cell proliferation and secretion of collagen by human-derived dermal fibroblasts [72]. In conclusion, the electrospun nanofibrous scaffolds with natural and synthetic polymers with L-ascorbic acid were characterized. Our results demonstrated that AA and HA in nanofibrous scaffold could enhance the chemical, mechanical and biological properties and the designed scaffolds can be used for skin tissue engineering.

Conclusion

In this study, PCL, PCL/HA nanofibers loaded with AA were successfully fabricated via electrospinning method and cross-linked through EDC. The SEM showed that smooth fibers were produced and average diameters ranging less than 180 nm. The crosslinked PCL/HA fibrous membranes displayed improved stability in PBS than non-crosslinked PCL/HA. Contact angle tests showed the PCL/HA and PCL/HA/AA scaffolds are moderately hydrophilic. Sustained release of AA in PCL/HA scaffolds was detected to progress over more than 100 hours. According to the cell culture experiments, PCL/HA and PCL/HA/AA scaffolds represented enhanced cell viability and contributed to the cell adhesion. Incorporation of these forms of ascorbic acid into biocompatible, biodegradable electrospun PCL/HA scaffolds could be useful for skin tissue engineering purposes.

References

1. M. H. Kailani, H. Jafar, and A. Awidi, *Skin Tissue Eng. Regen. Med.,* 163 (2016).
2. N. Bhardwaj, D. Chouhan, and B. B. Mandal, "Functional 3D Tissue Engineering Scaffolds", pp.345-365, Woodhead Publishing, 2018.
3. M. Janmohammadi and M. S. Nourbakhsh, *Int. J. Polym. Mater. Polym. Biomater.*, **68**, 527 (2018).
4. K. Ghosal, A. Chandra, G. Praveen, S. Snigdha, S. Roy, C. Agatemor, S. Thomas, and I. Provaznik, *Sci. Rep.*, **8**, 1 (2018).
5. M. M. Hasan, A. M. Alam, and K. A. Nayem, *Eur. Sci. J.*, **10**, 265 (2014).
6. N. Bhardwaj and S. C. Kundu, *Biotechnol. Adv.*, **28**, 325 (2010).
7. C. Tangsadthakun, S. Kanokpanont, N. Sanchavanakit, T. Banaprasert, and S. Damrongsakkul, *J. Metals, Mater. Min.*, **16**, 37 (2017).
8. S. P. Zhong, Y. Z. Zhang, and C. T. Lim, *Wiley Interdiscip. Rev.: Nanomed. Nanobiotechnol.*, **2**, 510 (2010).
9. A. Chaudhari, K. Vig, D. Baganizi, R. Sahu, S. Dixit, V. Dennis, S. Singh, and S. Pillai, *Int. J. Mol. Sci.*, **17**, 1974 (2016).
10. N. I. A. Mahboob Morshed, S. R. Chowdhury, and B. H. I. Ruszymah, *Regen. Res.*, **3**, 17 (2014).
11. K. Ghosal, M. S. Latha, and S. Thomas, *Eur. Polym. J.*, **60**,

58 (2014).
12. A. Arabi, E. Boggs, and M. Patel, *Surf. Innov.*, **2**, 47 (2014).
13. E. Luong-Van, L. Grøndahl, K. N. Chua, K. W. Leong, V. Nurcombe, and S. M. Cool, *Biomaterials*, **27**, 2042 (2006).
14. M. Chen, M. Chopra, and S. Bhowmick, *MRS Online Proceedings Library Archive*, 1235 (2009).
15. A. K. Ekaputra, G. D. Prestwich, S. M. Cool, and D. W. Hutmacher, *Biomaterials*, **32**, 8108 (2011).
16. E. Vatankhah, D. Semnani, M. P. Prabhakaran, M. Tadayon, S. Razavi, and S. Ramakrishna, *Acta Biomater.*, **10**, 709 (2014).
17. E. K. Brenner, J. D. Schiffman, E. A. Thompson, L. J. Toth, and C. L. Schauer, *Carbohydr. Polym.*, **87**, 926 (2012).
18. M. N. Collins and C. Birkinshaw, *Carbohydr. Polym.*, **92**, 1262 (2013).
19. K. Y. Lee, L. Jeong, Y. O. Kang, S. J. Lee, and W. H. Park, *Adv.Drug Deliv. Rev.*, **61**, 1020 (2009).
20. M. Arnal-Pastor, C. M. Ramos, M. P. Garnés, M. M. Pradas, and A. V. Lluch, *Mater. Sci. Eng.: C*, **33**, 4086 (2013).
21. A. L. McNulty, T. P. Vail, and V. B. Kraus, *Biochimica et Biophysica Acta (BBA)-Biomembranes*, **1712**, 212 (2005).
22. K. A. Naidu, *Nutr. J.*, **2**, 7 (2003).
23. D. J. MacKay and A. L. Miller, *Altern. Med. Rev.*, **8**, 359 (2003).
24. M. Stevanović, J. Savić, B. Jordović, and D. Uskoković, *Colloids Surf. B: Biointerfaces*, **59**, 215 (2007).
25. L. Avizheh, T. Peirouvi, K. Diba, and A. Fathi-Azarbayjani, *Ther. Deliv.*, **10**, 757 (2019).
26. R. Najafi-Taher, M.A. Derakhshan, R. Faridi-Majidi, and A. Amani, *RSC Adv.*, **5**, 50462 (2015).
27. A. Chanda, J. Adhikari, A. Ghosh, S. R. Chowdhury, S. Thomas, P. Datta, and P. Saha, *Int. J. Biol. Macromol.*, **116**, 774 (2018).
28. M. Hu, E. E. Sabelman, Y. Cao, J. Chang, and V. R. Hentz, *J. Biomed. Mater. Res. Part B: Appl.Biomater.*, **67**, 586 (2003).
29. A. C. Bean, A. J. Almarza, and K. A. Athanasiou, *Proc. Inst. Mech. Eng. H: J. Eng. Med.*, **220**, 439 (2006).
30. P. L. Lu, J. Y. Lai, D. H. K. Ma, and G. H. Hsiue, *J. Biomater. Sci., Polym. Ed.*, **19**, 1 (2008).
31. J. J. Young, K. M. Cheng, T. L. Tsou, H. W. Liu, and H. J. Wang, *J. Biomater. Sci., Polym. Ed.*, **15**, 767 (2004).
32. M. N. Collins and C. Birkinshaw, *J. Appl. Polym. Sci.*, **104**, 3183 (2007).
33. C. Pattamaprom, W. Hongrojjanawiwat, P. Koombhongse, P. Supaphol, T. Jarusuwannapoo, and R. Rangkupan, *Macromol. Mater. Eng.*, **291**, 840 (2006).
34. C. J. Luo, E. Stride, and M. Edirisinghe, *Macromolecules*, **45**, 4669 (2012).
35. Z. Wang, Y. Qian, L. Li, L. Pan, L. W. Njunge, L. Dong, and L.Yang, *J. Biomater. Appl.*, **30**, 686 (2016).
36. N. Mangır, A. J. Bullock, S. Roman, N. Osman, C. Chapple, and S. MacNeil, *Acta Biomater.*, **29**, 188 (2016).
37. S. N. Park, H. J. Lee, K. H. Lee, and H. Suh, *Biomaterials*, **24**, 1631 (2003).
38. J. F. Kirk, G. Ritter, I. Finger, D. Sankar, J. D. Reddy, J. D. Talton, C. Nataraj, S. Narisawa, J. L. Millan, and R. R. Cobb, *Biomatter*, **3**, e25633 (2013).
39. H. M. Liou, L. R. Rau, C. C. Huang, M. R. Lu, and F. Y. Hsu, *J. Nanomater.*, **2013**, 6 (2013).
40. N. Gokalp, C. Ulker, and Y. A. Guvenilir, *J. Polym. Mater.*, **33**, 87 (2016).
41. A. Abdolmaleki and Z. Mohamadi, *Colloid Polym. Sci.*, **291**, 1999 (2013).
42. S. H. Chen, C. H. Chen, K. T. Shalumon, and J. P. Chen, *Int. J. Nanomed.*, **9**, 4079 (2014).
43. N. Ashwinkumar, S. Maya, and R. Jayakumar, *RSC Adv.*, **4**, 49547 (2014).
44. H. Liu, K. Li, L. Lan, J. Ma, Y. Zeng, L. Xu, and D. Wu, *J. Mater. Chem. B,* **2**, 5238 (2014).
45. A. Umer, S. Naveed, N. Ramzan, M. S. Rafique, and M. Imran, *Matéria (Rio de Janeiro),* **19**, 197 (2014).
46. C. Y. Panicker, H. T. Varghese, and D. Philip, *Spectrochim. Acta Part A: Mol. Biomol. Spectrosc.*, **65**, 802 (2006).
47. R. Othayoth, P. Mathi, K. Bheemanapally, L. Kakarla, and M. Botlagunta, *J. Microencapsul.*, **32**, 578 (2015).
48. M. M. Sk and C. Y. Yue, *J. Mater. Chem. A*, **2**, 2830 (2014).
49. J. H. Yang, S. Y. Lee, Y. S. Han, K. C. Park, and J. H. Choy, *Bull. Korean Chem. Soc.*, **24**, 499 (2003).
50. T. Yokoyama, *KONA Powder and Particle J.*, **23**, 7 (2005).
51. E. Bayrak, B. Ozcan, and C. Erisken, *J. Polym. Eng.*, **37**, 99 (2017).
52. A. Diaconu, L. E. Nita, M. Bercea, A. P. Chiriac, A. G. Rusu, and D. Rusu, *Biochem. Eng. J.*, **125**, 135 (2017).
53. M. Van Beek, A. Weeks, L. Jones, and H. Sheardown, *J. Biomater. Sci., Polym. Ed*., **19**, 1425 (2008).
54. S. R. Son, N. T. B. Linh, H. M. Yang, and B. T. Lee, *Sci. Technol. Adv. Mater.*, **14**, 015009 (2013).
55. L. Li, Y. Qian, C. Jiang, Y. Lv, W. Liu, L. Zhong, K. Cai, S. Li, and L.Yang, *Biomaterials*, **33**, 3428 (2012).
56. C. Gandhimathi, X. H. E. Neo, P. Jayaraman, J. R. Venugopal, S. Ramakrishna, and S. D. Kumar, *J. Drug Metab. Toxicol*., **5**, 177 (2015).
57. S. Xu, J. Li, A. He, W. Liu, X. Jiang, J. Zheng, C. C. Han, B. S. Hsiao, B. Chu, and D. Fang, *Polymer*, **50**, 3762 (2009).
58. T. G. Kim, H. J. Chung, and T. G. Park, *Acta Biomater.*, **4**, 1611 (2008).
59. D. R. Figueira, S. P. Miguel, K. D. de Sá, and I. J. Correia, *Int. J. Biol. Macromol.*, **93**, 1100 (2016).
60. M. Jaganjac, L. Milković, A. Čipak Gašparović, M. Mozetič, N. Recek, N. Žarković, and A. Vesel, *Mater. Tehnol*., **46**, 53 (2012).
61. M. Lebourg, J. R. Rochina, T. Sousa, J. Mano, and J. L. G. Ribelles, *J. Biomed. Mater. Res. Part A*, **101**, 518 (2013).
62. B. Tavsanli and O. Okay, *Eur. Polym. J.*, **94**, 185 (2017).
63. B. R. Mintz and J. A. Cooper Jr, *J. Biomed. Mater. Res.*

Part A, **102**, 2918 (2014).
64. K. Ghosal, S. Thomas, N. Kalarikkal, and A. Gnanamani, *J. Polym. Res.*, **21**, 410 (2014).
65. X. Zhao, Y. S. Lui, P. W. J. Toh, and S. C. J. Loo, *Materials*, **7**, 7398 (2014).
66. S. Yan, Q. Zhang, J. Wang, Y. Liu, S. Lu, M. Li, and D. L. Kaplan, *Acta Biomater.*, **9**, 6771 (2013).
67. J. H. Collier, J. P. Camp, T. W. Hudson, and C. E. Schmidt, *J. Biomed. Mater. Res.*, **50**, 574 (2000).
68. K. Ghosal, A. Manakhov, L. Zajíčková, and S. Thomas, *Aaps Pharmscitech*, **18**, 72 (2017).
69. S. Deepthi, K. Jeevitha, M. N. Sundaram, K. P. Chennazhi, and R. Jayakumar, *Chem. Eng. J.*, **260**, 478 (2015).
70. K. M. Choi, Y. K. Seo, H. H. Yoon, K. Y. Song, S. Y. Kwon, H. S. Lee, and J. K. Park, *J. Biosci. Bioeng.*, **105**, 586 (2008).
71. J. Y. Zhang, B. A. Doll, E. J. Beckman, and J. O. Hollinger, *Tissue Eng.*, **9**, 1143 (2003).
72. S. Sridhar, J. R. Venugopal, and S. Ramakrishna, *J. Biomed. Mater. Res. Part A*, **103**, 3431 (2015).